PNAS
www.pnas.org

Supplementary Information for

Altered interplay between endoplasmic reticulum and mitochondria in Charcot-Marie-Tooth type 2A neuropathy

Nathalie Bernard-Marissal, Gerben van Hameren, Manisha Juneja, Christophe Pellegrino, Lauri Louhivuori, Luca Bartesaghi, Cylia Rochat, Omar El Mansour, Jean-Jacques Médard, Marie Croisier, Catherine Maclachlan, Olivier Poirot, Per Uhlén, Vincent Timmerman, Nicolas Tricaud, Bernard L. Schneider, Roman Chrast

Corresponding author:
Roman Chrast
Email: roman.chrast@ki.se

Correspondence may also be addressed to:

Nathalie Bernard-Marissal
Email: nathalie.bernard.1@univ-amu.fr

Bernard L. Schneider
Email:bernard.schneider@epfl.ch

This PDF file includes:

www.pnas.org/cgi/doi/10.1073/pnas.1810932116

Supplementary Information Materials and Methods

Animals

In vivo work was performed using the mouse strain B6;D2-Tg (Eno2-MFN2*R94Q) L51Ugfm/J previously described (1) (alternative name *MitoCharc1*, purchased from Jackson Laboratories, stock No: 012812). Animals were maintained as heterozygous by crossing B6;D2-Tg $^{(Eno2\text{-}MFN2*R94Q)/-}$ males with B6;D2F1 females (Janvier). Offspring was genotyped using a standard PCR reaction with the following primers recommended by Jackson Laboratories: 10453: 5' ATG CAT CCC TTA AGC AC 3', 10454: 5' CCA GAG GGC AGA ACT TTG 3'; oIMR8744: 5' CAA ATG TTG CTT GTC TGG TG 3', oIMR8745: 5' GTC AGT CGA GTG CAC AGT TT 3'.

Neuronal cultures were prepared from embryos (Swiss Rj Orl mouse strain, purchased from Janvier) collected at gestational day 12.5. Animals were housed in an animal facility with 12 h light / 12 h dark environment, and *ad libitum* access to water and normal diet. All experiments were done in accordance with Swiss legislation and the European Community Council directive (86/609/EEC) for the care and use of laboratory animals and were approved by the Veterinarian Office of the canton of Vaud and a local ethics committee.

Behavioral Studies

In accordance with dominant CMT2A inheritance, all animals studies were performed on heterozygote B6;D2-Tg $^{(Eno2\text{-}MFN2*R94Q)/-}$ mice (described here as *CMT2A Tg*) or matched control animals (described as wild-type).

Muscle strength was evaluated with the grid test as previously described (2). After two days of training, the ability of mice to lift grids of 20, 30 and 40 g was measured three times for a maximum of 30 sec each, and the best score was recorded. Muscle strength score value corresponds to the sum of the holding times for each grid multiplied by the weight of each grid. Sensory function was evaluated using the plantar Von Frey test. The touch sensitivity following mechanical stimulation of the mouse hindpaw was measured using a dynamic plantar aesthesiometer (Ugo Basile). For habituation, mice were placed into the compartment for 45 min before the experiments. A 0.5-mm von Frey filament was used to exert increasing forces on paw and the force exerted at the time of paw withdrawal was automatically recorded. Both right and left hind paws were stimulated three times and the values averaged. Locomotion was evaluated by the rotarod and CatWalk tests. Latency to fall was tested on an accelerating rotarod (4-40 rpm) with a maximum latency of 300 sec. Each mouse was tested twice and the best score was kept (3). Experiments on the CatWalk walkway apparatus (Noldus, The Netherlands) were performed as described in (4). Before recording footprints, mice were acclimated and trained to walk on the CatWalk system for two days. A cylinder was placed at the level of the goal box as a source of motivation for a successful run. During testing session, the animals walked back and forth on the glass plate for 10 runs and a minimum of 2-3 completed runs were collected. Locomotion parameters were analysis with the CatWalk XT 8.1 software to provide a global footprint analysis for each paw. For each mouse, the values of the completed runs were averaged.

The following parameters are presented: *Intensity-based parameters* which represent the mean pressure of a paw on the glass plate, i.e. mean intensity, maximum

intensity of a paw during maximum contact, average intensity of a paw during maximum contact, all expressed as arbitrary units (a.u.). *Paw-size parameters* which represent the mean length and width of a complete print (expressed in cm) and the print area of complete prints (expressed in cm^2). *Gait/posture parameters* include stance, i.e. the duration of contact of a paw with the glass plate (expressed in s), and swing, which represents the interval of no contact of a paw with the glass plate (expressed in sec). Step cycle refers to the duration between two placements of the same paw (expressed in sec). Dual stance is defined as time of simultaneous contact of either hind or front paws with the glass plate (expressed in sec). In the second instance of the step cycle, it is defined as terminal dual stance. Duty cycle mean represents the percentage of stance in a step cycle (stance/(stance+swing)). The support variable indicates the percentage of a run with a specific number of paws on the glass plate ('support three': three paws simultaneously in contact with the walkway). *Coordination parameters* represent phase dispersions and couplings that characterize the temporal relationship between placements of two paws (anchor paw and target paw) within a step cycle. Values are expressed as percentage and are a measure of inter-paw coordination.

Electromyography

CMAP amplitude was recorded in isoflurane-anesthetized mice from two electrodes placed in the belly of the *tibialis anterior* muscle. The sciatic nerve was stimulated non-specifically by two electrodes placed on the lumbar vertebra of isoflurane-anesthetized mice (1 pulse of 0.2 ms, current 20 mA). Consequent muscle depolarization was intramuscularly recorded with an electromyography apparatus (AD Instruments, Oxford, UK).

Fibroblast lines

Skin biopsies were obtained from two normal controls and two CMT2A patients (PN198.1 and PN198.3) with a p.Arg94Gln missense mutation in the Mitofusin 2 gene (*MFN2*). Clinical, electrophysiological and neuropathological characteristics of these patients were reported by (5). Five-millimeter punch forearm glabrous skin biopsies were obtained after local anesthesia and brought in 15 ml of F-12 (Ham) nutrient mixture + L-glutamine and kept overnight at 24 °C before further processing for cell culture. With a sterile disposable scalpel, the biopsies were chopped into 1 mm pieces, divided into two parts and cultured in a standard incubator at 37 °C, with 5 % CO_2 for 4–5 weeks using complete culture medium: F-12 (Ham) nutrient mixture (Gibco, Invitrogen, supplemented with 15 % fetal bovine serum, 1 % penicillin/streptomycin, 1 % glutamine). Primary fibroblast cells migrating out of the biopsies were monitored daily and every two days the culture medium was refreshed. Confluent culture dishes were expanded in DMEM medium (ThermoFisher Scientific) supplemented with 10 % fetal bovine serum (ThermoFisher Scientific) in a 37 °C and 5 % CO_2 atmosphere. Appropriate consent was obtained from participants and the Institutional Review Board from the University of Antwerp approved the study.

MFN1 expression in fibroblast lines

Controls and CMT2A patient-derived fibroblasts were transiently transfected with pcDNA3.1-CMV-*MFN1*-Myc plasmid (Addgene plasmid # 23212). 48 hours after transfection the cells were fixed with 4% PFA in PBS and used for the proximity ligation assay. In order to identify the cells overexpressing MFN1, an anti-myc antibody (1:1000, Cell Signaling) has been used.

Constructs and production of AAV vectors

Plasmid containing Myc-Human *MFN2* was generously provided by Dr. Darren Moore. Myc-hMFN2 cassette was subcloned in a pAAV-hsyn-MCS plasmid for expression under the control of the hSyn1 promoter. Arginine-to-glutamine substitution at position 94 of *MFN2* was generated using Quickchange site-directed mutagenesis kit (Agilent). A similar construct was generated for expression of Myc-Human *MFN1* (NM_033540.2, tebu-bio). For AAV2/6 vector production, pAAV plasmids (pAAV-hsyn-hMFN2^{WT}, pAAV-hsyn-hMFN2^{R94Q}, pAAV-hsyn-hMFN1, pAAV-hsyn-GFP and pAAV-CMV-GFP) were co-transfected with pDP6 helper plasmid into HEK293-AAV cells (Agilent). Cells were lysed 72 h after transfection and viral particles were purified using iodixanol gradient followed by separation on heparin affinity columns. The infectivity titer of each virus (expressed as Transduced Units/mL) was determined following infection of HEK293T cells by real-time PCR using primers for WPRE element (forward: 5' CCG TTG TCA GGC AAC GTG 3', reverse: 5'AGC TGA CAG GTG GTG GCA AT 3', probe: FAM-TGC TGA CGC AAC CCC CAC TGG T-BHQ1) and human albumin (forward: 5' TGA AAC ATA CGT TCC CAA AGA GTT T 3', reverse: 5' CTC TCC TTC TCA GAA AGT GTG CAT AT 3', probe: FAM-TGC TGA AAC ATT CAC CTT CCA TGC AGA-TAMRA).

Primary neuronal cultures

Motor and sensory neurons cultures were prepared from E12.5 mouse embryos as previously described (2). Briefly, dissected spinal cords and DRGs were collected and dissociated mechanically after trypsin treatment. Sensory neurons were then directly plated on glass coverslips coated with poly-ornithine/laminin in Neurobasal medium containing 4 g/l D-glucose, 2 % of B27 (Invitrogen), 2 mM L-glutamine and 50 ng/ml NGF (AbD Serotec). Motoneurons were separated according to their large size by a density gradient of iodoxanol (5.2%), and plated after centrifugation in supplemented Neurobasal medium containing 2 % horse serum, 2 % B27, 0.025 mM L-glutamine, 25 mM glutamate, 25 mM mercaptoethanol and a cocktail of neurotrophic factors (1 ng/ml BDNF, 200 pg/ml GDNF and 10 ng/ml CNTF; R&D Systems).

For analysis of neuronal survival, mitochondrial transport and ER stress, neuronal cultures were infected with AAV6-hsyn-MFN2^{WT} or AAV6-hsyn-MFN2^{R94Q} (10 TU/cell) 48 h after plating and analyzed at indicated time points (4, 6 or 8 days post-infection (dpi)). For quantification of neuritic length, neurons were co-infected with AAV2/6-hsyn-MFN2^{WT} or AAV2/6-hsyn-MFN2^{R94Q} (10 TU/cell) and AAV2/6-CMV-GFP (1 TU/cell) to label neuronal processes with GFP.

Reagents

Mitotracker Red CMXRos was purchased from Life technologies. Pre-084 was purchased from Tocris Biosciences and used at 50 nM on primary neurons. For *in vitro*

experiments, neurons were treated with 5 µM of Salubrinal (Sigma Aldrich). For *in vivo* experiments, Salubrinal diluted in sterile saline solution was intraperitoneally injected daily at a dose of 1 mg/kg.

Immunocytochemistry

Neuronal and fibroblasts cultures collected at indicated time-points were fixed for 20 min in 4 % paraformaldehyde (PFA), and washed twice with PBS. Coverslips were incubated for 1 h at room temperature in blocking solution (PBS with 2 % BSA, 2 % heat-inactivated horse serum, 0.1 % Triton X-100) and overnight at 4 °C with the following primary antibodies: rabbit anti-myc (Cell signaling, 1/250), rabbit anti-IP3R (Abcam, 1/250), mouse anti-VDAC1 (Abcam, 1/250), rabbit anti-peripherin (Millipore, 1/1000), rabbit anti-GFP (Invitrogen, 1/500), rabbit anti-phospho-eIF2α (Invitrogen, 1/250), mouse anti-non-phosphorylated neurofilament H (SMI32, Biolegend, 1/500) and anti-mouse neurofilament 200 (Sigma Aldrich, 1/500). Coverslips were next incubated with appropriate fluorochrome-conjugated secondary antibodies (Molecular Probes) and mounted in Mowiol Medium. Fluorescence was observed under a Zeiss Axioplan fluorescence microscope with a 63x objective and images were analyzed using Fiji or Axiovision software.

Proximity Ligation Assay

Fixation and blocking were performed as described for immunocytochemistry. To label MAM, neurons or fibroblasts were incubated overnight at 4 °C with rabbit anti-IP3R and mouse anti-VDAC1 primary antibodies in the antibody reagent buffer provided in the proximity ligation assay (PLA) kit (Duolink, Sigma-Aldrich). Cells were then incubated with the anti-mouse minus and anti-rabbit plus probes in the antibody reagent buffer for 1 h at 37 °C. If the antigens of interests are closer than 40 nm connector oligonucleotides can hybridize with the probes and after ligation, the signal is enhanced by rolling circle amplification. Coverslips were mounted in Vectashield mounting medium containing DAPI. We used the red Duolink detection fluorophore. The fluorescent spots corresponding to the MAM signal were imaged using a Zeiss Axioplan fluorescence microscope under a 40x objective and analyzed using Fiji software.

Calcium Imaging

Quantitative changes of $[Ca^{2+}]i$ in sensory and motor neurons were monitored using a Fura-Red acetoxymethyl ester (AM) dye (Invitrogen) that allows effective ratiometric fluorescence measurements. At 6 dpi, neurons were rinsed with an external solution containing (in mM):150 NaCl, 2 KCl, 2 $MgCl_2$, 2 $CaCl_2$, 10 HEPES, and 10 glucose, pH 7.4, and incubated in the same solution containing 4 µM Fura-Red AM for 30 min in the dark at 20 °C. The dye was washed off and the coverslips were kept in the dark for a further 30 min at RT to allow de-esterification of the dye. To selectively visualize Ca^{2+} in motor and sensory neurons, we acquired fluorescent images of Fura-Red. Fura-Red was alternately excited at 440 nm and 490 nm using a xenon light source (Sutter Instruments), and emission collected at 660 nm using a CCD camera (Hamamatsu). During experiments, neurons were continuously perfused with external solution. Fifteen seconds after beginning the experiment, neurons were activated by a brief (8 sec) application of the external solution containing 25 mM KCl (replacing

equimolar amount of NaCl in the external solution), applied via a fast perfusion system. After KCl application, the neurons were perfused with the KCl-free solution for an additional 3 min to let them recover. To analyze $[Ca^{2+}]i$, we drew regions of interest around neurons and then applied these regions of interest for analysis of Fura-Red images using simplePCI software. $[Ca^{2+}]i$ values are presented as the 490/440 nm ratio.

Fibroblasts were loaded with the Ca^{2+}-sensitive fluorescence indicator Fluo-4/AM (5 µM; Invitrogen) at 37 °C with 5 % CO_2 for 30 min in a Krebs-Ringer buffer containing (in mM) 119 NaCl, 5 KCl, 1 CaCl2, 1 MgCl2, 1 NaH2PO4, 20 Hepes (pH 7.4), and 10.0 glucose prior to experiments. Ca^{2+} measurements were carried out in Krebs-Ringer buffer at room temperature with a cooled CCD camera (Photometrics QuantEM) mounted on an upright microscope (Axio Examiner D1, Zeiss) equipped with a 20x/0.8NA dipping lens (Carl Zeiss, Jena, Germany). All drugs were bath applied. Excitation was set at 488 nm and the sampling frequency was set to 1Hz (1 image every second). MetaFluor software (Molecular Devices) was used to control all devices. Analysis of the acquired fluorescent images were performed off line using Fiji (6) and custom MATLAB (MathWorks Inc.) scripts. Changes in fluorescence intensity over mean fluorescence were calculated for each ROI over the entire time course.

Mitochondrial axonal transport

AAV2/9-CAG-mitoDsred2 (1 µl) were transdermally introduced via a thin glass needle into the spinal cord of 1-day-old mice using a micromanipulator with short pressure pulses using a Picopump (World Precision Instrument) coupled to a pulse generator. One month after injection, mice were anesthetized for 5 min in an induction box (World Precision Instruments) with a constant flow (1.5 l/min) of oxygen + 5 % isoflurane. Anesthesia was then maintained with a mask delivering 2 % isoflurane at 0.8 l/min. The mouse was placed in a silicone mold on its belly, shaved and cleaned on the back of the right thigh and the right paw was stabilized using small pins. Skin and fat tissue were cut out using scissors and the sciatic nerve was gently detached from connective tissue. The nerve was lifted using a plastic strip inserted below and kept in sterile PBS buffer to prevent drying. At that point, the mouse was placed on a motorized platform. Then a glass coverslip was placed on top of the nerve and a drop of deionized water or oil was used to immerse the 20x or 63x objective lens, respectively as previously described (7). All time-lapse images were obtained with a multiphoton microscope LSM 7 MP OPO (Zeiss France) coupled to a dark microscope incubator in which the temperature was maintained at 37 °C. Mitochondria images were acquired by time-lapse recording, varying from one image every min to one image every 5 min during 1 h. Each image represents a stack of 10 scans over 40 µm of depth. Images were acquired for each time point using 920 nm wavelength as excitation light (7). To analyze mitochondrial parameters in peripheral axons, we used ImageJ software to project parts of the axon, located in different Z-layers, in a single maximum intensity image. The multiple time-point images were aligned using the Template Matching plugin in ImageJ. To measure size of a single mitochondrion, we drew a line along the axis of the smallest isolated object and measured the line length using Image J software. To measure the size of mitochondrial clusters we drew a similar line through individually identified objects. To measure mitochondrial speed, we defined a ROI encompassing individual mitochondrion using Image J and the movement of each ROI was calculated using the MTrackJ plugin

of Image J software. Speed is expressed as µm/min. 3D images were reconstructed using Bitplane Imaris 8.3.1. software.

Immunohistochemistry

Mice were sacrificed with an overdose of pentobarbital (150 mg/kg) and then transcardially perfused with PBS followed by 4 % PFA. Spinal cord and muscles were dissected out. Spinal cords were postfixed during 2-3 h at 4 °C whereas muscle samples were post-fixed during 20 min. Samples were incubated in 25 % sucrose solution at 4 °C for 24 h. Tissues were embedded in optimal cutting temperature compound (OCT, Tissue-Tek) and stored at -80 °C before processing. Twenty µm-thick spinal cord sections were cut and conserved free floating in azide/PBS solution. Spinal cord sections were then mounted on superfrost plus slides (Thermo Scientific), washed with PBS and incubated in blocking solution (4 % BSA, 10 % heat inactivated goat or donkey serum, 0.2 % of Triton-X100) for 1 h at room temperature, before incubation with the following antibodies: mouse anti-ATF6 (Novus Biologicals, 1/150), rabbit anti-P-eIF2α (Invitrogen, 1/150), mouse anti-PDI (Abcam, 1/150), mouse anti-NeuN (Millipore, 1/500) and goat anti-ChAT (Millipore, 1/500). Immunodetection was made with either appropriate fluorochrome-conjugated secondary antibodies (Alexa Fluor 488 or Cy3, Molecular Probes) or secondary biotinylated antibody (Vector BA-9500) combined with Vectastain ABC-Elite kit (Vector Labs) and 0.05 % 3,3′-diaminobenzidine (DAB, Sigma Aldrich) staining. Fluorescent-labelled sections were mounted in Mowiol mounting medium and imaged on Axioplan fluorescence microscope (Zeiss) with a 20x objective. Integrated density of fluorescence signal was analyzed in 15-20 motoneurons per animal using Fiji software and expressed as a ratio Protein-of-interest/NeuN. Motoneuron survival was directly evaluated under a transmitted light Olympus CX41 microscope. The nuclear versus cytoplasmic ATF6 staining was determined directly from the stainings as previously described (8). Cells with a nucleus clearly delineated by a nuclear ATF6 staining more intense than the cytoplasmic staining were scored as "nuclear ATF6 staining" (see red arrow in Fig. 4E), while cells with diffuse staining mainly visible throughout the cytoplasm (see white arrow in Fig. 4E) where scored as "cytoplasmic ATF6 staining".

Neuromuscular Junctions (NMJ) occupancy was quantified on 25-µm and 16-µm thick longitudinal tibialis and soleus sections, respectively. Muscle sections were incubated overnight at 4 °C in blocking solution (2 % BSA, 10 % NGS, 0.1 % Triton and PBS) with mouse anti-SV2 (Developmental Hybridoma Bank, 1/50). Sections were next incubated with goat anti-mouse IgG1 Cy3-conjugated antibody (Jackson ImmunoResearch, 1/500) and Bungarotoxin-488 (Molecular Probes, 1/500), and mounted in Mowiol mounting medium. NMJ were imaged on Axioplan fluorescence microscope (Zeiss) with a 20x objective.

Western blot

Western blots were done on lysates from lumbar spinal cord dissected from 12-month-old wild-type or *CMT2A Tg* mice. Samples were lysed in RIPA buffer (abcam, ab1560034) and protein concentration was determined using the BCA kit (Pierce, ThermoFischer Scientific). Protein samples were then separated using NuPage 12% Bis-Tris gels (ThermoFischer Scientific) and blotted to nitrocellulose membrane (GE

healthcare life science, Germany). After incubation in blocking buffer (Tebu-Bio-Rockland MB-070), membranes were incubated with the following antibodies: goat anti-SIGMAR1 1/500 (Santa Cruz), rabbit anti VAPB 1/500 (Novus Biologicals) and goat anti-GAPDH 1/1000 (Santa-Cruz Biotechnology, #sc-48167). Blots were then incubated with donkey anti-rabbit IRDye 800 and donkey anti-goat IRDye 680, (Li-Cor Biosciences), diluted at 1/10000. Acquisition of the blots was done using the LI-COR Odyssey system by following recommendations of the manufacturer. Immunoblot images were quantified using the software ImageJ and normalized relative to GAPDH levels.

Electron microscopy

Animals were sacrificed with an overdose of pentobarbital (150 mg/kg) and transcardially perfused with PBS followed by 2 % PFA/2.5 % Glutaraldehyde in 0.1 M PBS. Spinal cords, sciatic nerves and dorsal and ventral roots were dissected out and kept in fixative solution at 4 °C overnight. Coronal 80-µm thick sections were obtained from the lumbar spinal cord and distal part of the sciatic nerve using a vibratome. Sections were washed in 0.1 M cacodylate buffer, post-fixed in 1.5 % potassium ferrocyanide, followed by 1 % osmium tetroxide, and stained with 1 % uranyl acetate. Sections were dehydrated in a graded alcohol series, embedded in Durcupan resin (Fluka) to finally be mounted on coated glass slides and heated up at 65 °C overnight. Ultra-thin sections were processed and photographs were obtained using transmission FEI Tecnai Spirit BioTWIN microscope.

The number of mitochondria apposed to ER, forming a MAM, was evaluated in the lumbar spinal cord of 12 month-old WT (n=33 motoneurons from 3 mice) and *CMT2A Tg* mice (n=33 motoneurons from 3 mice). Length of MAM was quantified in the same cells by measuring the length of the mitochondrial surface associated with the ER (<30 nm) reported to the circumference of each mitochondria and the proportions of the mitochondrial surface (circumference) as previously described (9).

Dorsal and ventral roots were post-fixed 2 h in fixative solution, washed in 0.1 M cacodylate buffer and incubated for 4 h in 1 % OsO4 (Fluka). Tissues were then rinsed, dehydrated and embedded in epoxy 812-Araldite (Sigma Aldrich). Semi-thin (0.5 mm) cross-sections were stained with 1 % toluidine blue and digitalized using Axioskop 40 with AxioCam MRc5 (Zeiss). Axon number was evaluated with Fiji software.

Statistical analyses and experimental design

Animals were matched by gender, genotype, age and weight. Mice were randomly assigned to experimental groups and all behavioral experiments as well as processing and analyzes of the tissues were performed in blind.

Size of the cohort for behavioral studies was estimated based on previous experiments using the *CMT2A Tg* model (1). We analyzed animals at the age of 6 and 12 months (5 males and 6 females for WT, 4 males and 8 females for *CMT2A Tg*) in rotarod, Von-Frey and grid tests. Additional mice were analyzed in the catwalk and rotarod tests at 6 months (4 males and 6 females for WT and 6 males and 5 females for *CMT2A Tg*) and 12 months of age (3 males and 3 females for WT and 6 males and 5 females for *CMT2A Tg*). In the catwalk paradigm, some mice (3 WT at 6 months of age and 2 WT and 2 *CMT2A Tg* at 12 months of age) did not move on the walkway and were hence excluded from the study.

For histology, we analyzed at least 3 mice per condition. *In vitro* results display the data averaged from at least 3 independent cultures. For behavioral studies, we performed either two-tailed student's t-test, one-way, two-way ANOVA or repeated-measures two-way ANOVA with Sidak, Tukey's or Newman-Keuls post-hoc tests, depending on the experimental design. Significance of the results for histology, electron microscopy, *in vivo* mitochondrial transport and primary cultures was evaluated with one-way, two-way ANOVA or two-tailed student's t-test according to experimental design. In figures 7F and 7G, non-parametric Kruskal-Wallis test with Dunn's post-hoc test was applied as the values did not follow normal distribution (D'Agostino and Pearson normality test). Statistical analyses were performed using the GraphPad Prism or Statistica software. All data are presented as mean ± standard error of the mean (sem) or using box-and-whisker plots (showing median, first and third quartiles and minimal/maximal values). The alpha level of significance was set at 0.05. Levels of significance are indicated as follows: *$p<0.05$, **$p<0.01$, ***$p<0.001$ and ****$p<0.0001$.

Supplementary Information – Figures

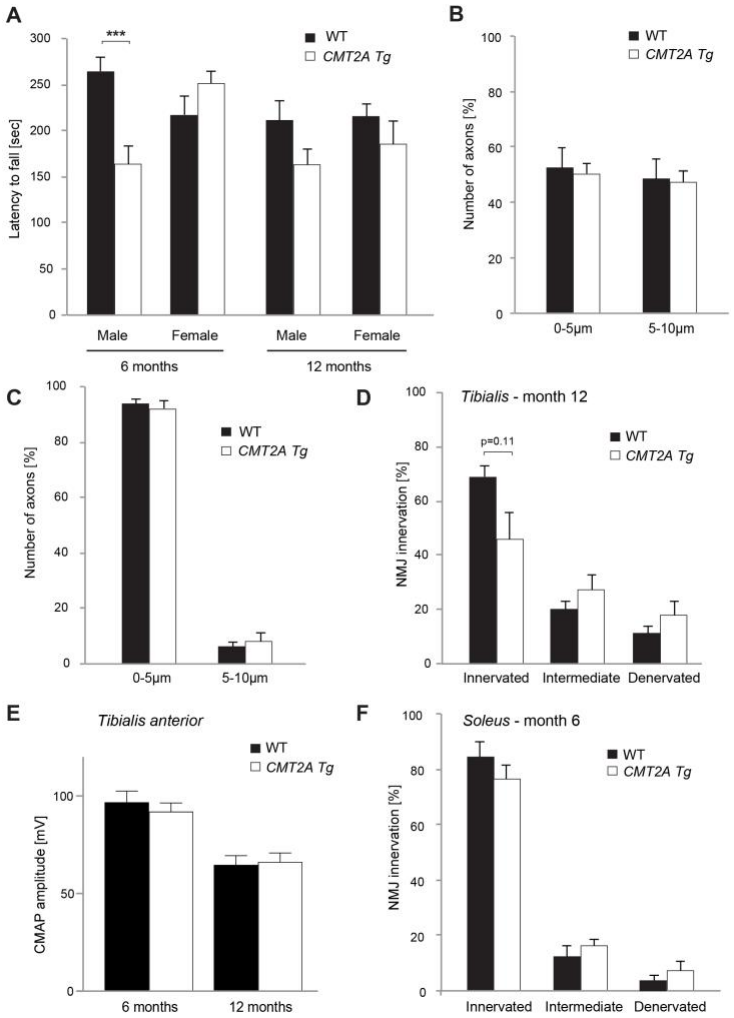

Fig. S1. *CMT2A Tg* mice display locomotion defects but no proximal axonal degeneration or tibialis muscle denervation

(A) Evaluation of motor function with rotarod test at 6 months (WT: n=21; *CMT2A Tg*: *n*=23) and 12 months of age (WT: n=17; *CMT2A Tg*: n=19). Statistical analysis: repeated-measures three-way ANOVA (group x gender x time) with Newman-Keuls post-hoc test. Note the significant loss of performance in 6 month-old male *CMT2A Tg* mice. **(B)** Number of motor axons in ventral roots of 12 month-old WT (n=2) and *CMT2A Tg* (n=3) mice. Axons were classified according to small (<5 µm) and large (>5 µm) calibers. Statistical analysis: two-tailed unpaired student's t-test. **(C)** Number of sensory axons in dorsal roots of 12 month-old WT (n=3) and *CMT2A Tg* (n=3) mice. Axons were classified according to small (<5 µm) and large (>5 µm) calibers. Statistical analysis: two-tailed unpaired student's t-test. **(D)** Levels of NMJ occupancy in the *tibialis* muscle at 12 months of age in WT (n=5) and *CMT2A Tg* mice (n=6). Statistical analysis: two-tailed unpaired student's t-test. **(E)** Electromyography recordings of the compound muscle action potential (CMAP) in the *tibialis anterior* muscle at 6 and 12 months of age

in WT (n=11) and *CMT2A Tg* mice (n=11). Statistical analysis: two-way ANOVA. **(F)** Levels of NMJ occupancy in the soleus muscle at 6 months of age in WT (n=3) and *CMT2A Tg* mice (n=3). Statistical analysis: two-tailed unpaired student's t-test. ***$P < 0.001$.

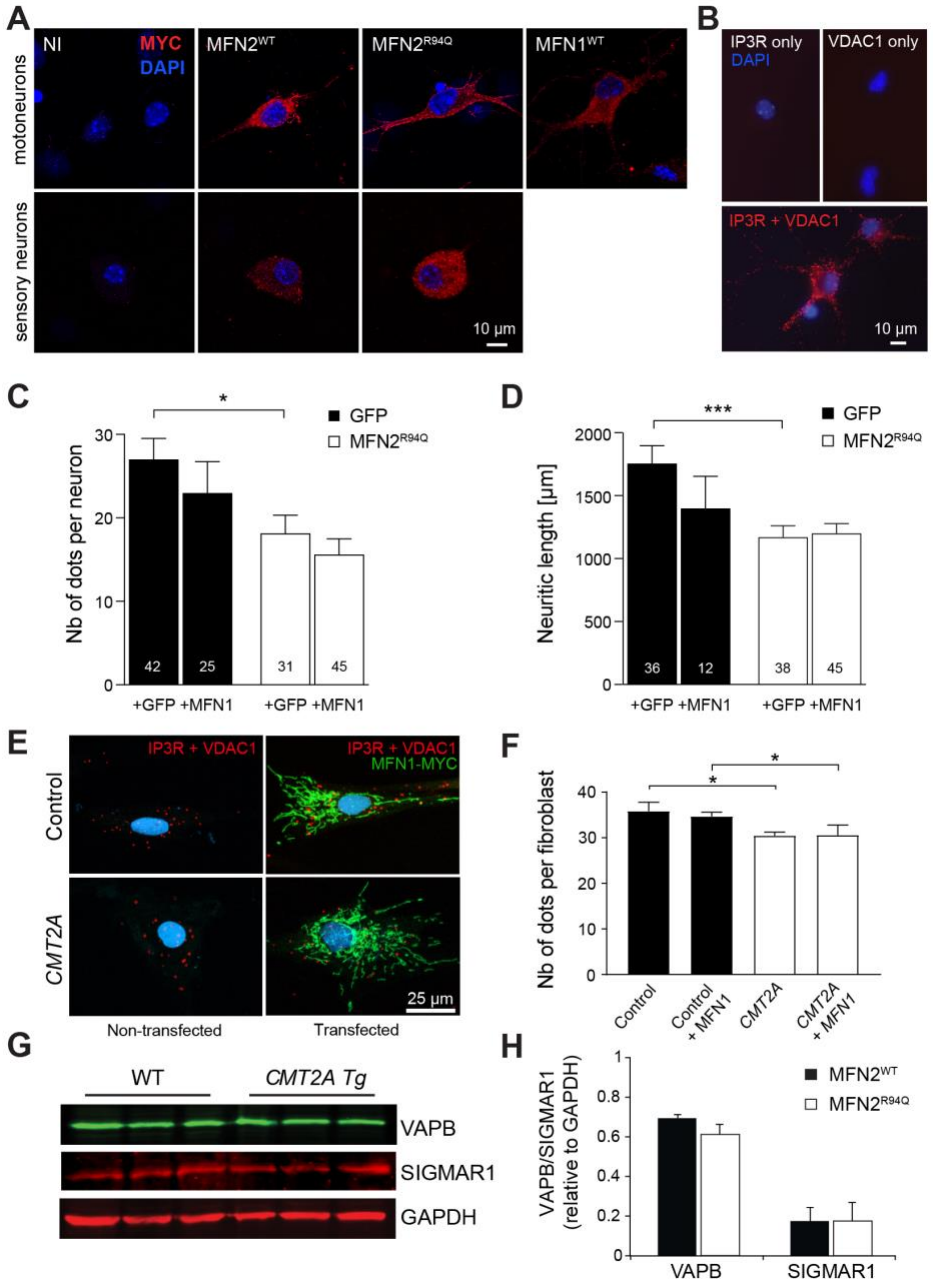

Fig. S2. Characterization of consequences of the overexpression of MFN2^{WT} or MFN2^{R94Q} in motor and sensory neurons

(A) Primary cultures of motor and sensory neurons were infected with AAV6-hsyn-hMFN2^{WT}, AAV6-hsyn-hMFN2^{R94Q}, or AAV6-hsyn-hMFN1^{WT}. Expression of MYC-tagged-MFN was revealed at 6 dpi with anti-myc staining. **(B)** As a control for specificity of antibodies used for proximity ligation assay, the experiment was performed without VDAC or IP3R antibody. No signal was detected under these conditions as compared to experiment performed in presence of both antibodies (IP3R + VDAC1). **(C, D)** Effects of co-expressing MFN1 (6 TU per cell) in motoneurons transduced with either

AAV6-hsyn-GFP or AAV6-hsyn-hMFN2^{R94Q} (6 TU per cell). **(C)** Proximity ligation assay shows no difference in the number of ER-mitochondria contacts in response to MFN1 overexpression. **(D)** Measurement of neurite length shows no rescue effect of MFN1 on the neurite shortening induced by MFN2^{R94Q}. Statistical analysis for C and D: two-way ANOVA with Sidak's post-hoc test for multiple comparisons. The number of replicates (motoneurons) obtained from 3 independent cultures is indicated in each bar. **(E)** Examples of control and CMT2A fibroblasts transfected or not with MFN1-MYC construct and analyzed by proximity ligation assay. **(F)** Quantification of ER-mitochondria contacts in control and CMT2A patient-derived fibroblasts transfected or not with MFN1-MYC construct (from n=3 independent transfection experiments). **(G-H)** Western blot on spinal cord extracts from 12 month-old WT (n=3) and 12 month-old *CMT2A Tg* (n=3) mice. **(G)** Proteins levels of two MAM proteins: VAPB and SIGMAR1 and GAPDH as a reference protein. **(H)** Levels of expression of VAPB and SIGMAR1 relative to GAPDH. Values are expressed as mean intensity ratio (protein of interest/GAPDH) ± sem (from n=3 animals). Statistical analysis: two-tailed unpaired student's t-test. *$P < 0.05$, ***$P < 0.001$.

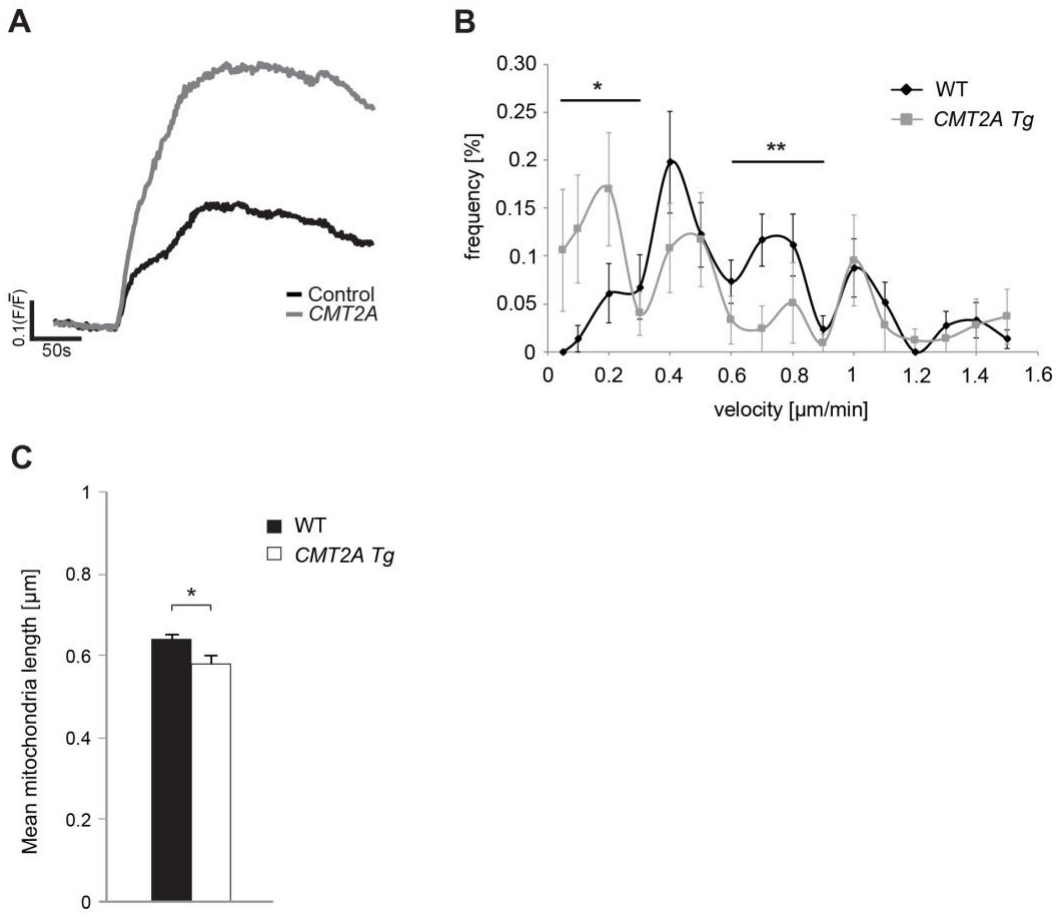

Fig. S3. Characterization of parameters related to ER and mitochondria biology
(**A**) Example of a recording obtained in a fibroblast exposed to CCCP (2µM). Calcium dynamics are expressed as the ratio of fluorescence intensity (F) divided by the mean fluorescence ($\bar{F}$) and represented as arbitrary units. (**B**) Velocity histogram showing mitochondrial transport in sciatic nerve axons of 1-month-old WT (n=24 axons from 7 mice) and *CMT2A Tg* (n=12 axons from 6 mice) mice. Mitochondria are classified according to fast (>0.9 µm/min), medium (>0.6 and <0.9 µm/min), slow (>0.3 and <0.6 µm/min) and very slow (<0.3 µm/min) transport velocities. Statistical analysis: repeated-measure two-way ANOVA. **(C)** Electron microscopy assessment of mitochondrial length in lumbar spinal cord motoneurons of 12 month-old WT (n=76 mitochondria from 5 mice) and *CMT2A Tg* mice (n=76 mitochondria from 5 mice). Statistical analysis: two-tailed unpaired student's t-test. **P* < 0.05, ***P* < 0.01.

Table S1

Parameters	6 months-old		
Paw intensity measures	**WT**	***CMT2A Tg***	***P-value***
Right forepaw Max contact max intensity (a.u)	196.6 ± 2.4	183.1 ± 2.9	0.001
Right forepaw Max intensity mean (a.u)	201.5 ± 1.9	191.7 ± 2.6	0.005
Right forepaw Mean intensity (a.u)	174 ± 3	161.9 ± 3	0.007
Left forepaw Mean intensity (a.u)	172 ± 3.7	162.4 ± 2.5	0.03
Paw size			
Right forepaw Print length mean (cm)	1.03 ± 0.018	0.97 ± 0.014	0.009
Right forepaw Print width mean (cm)	0.93 ± 0.02	0.86 ± 0.02	0.023
Right forepaw Print area mean (cm^2)	0.58 ± 0.02	0.51 ± 0.014	0.013
Gait/Posture			
Right forepaw Terminal dual stance (sec)	0.036 ± 0.005	0.057 ± 0.007	0.046
Left forepaw Duty cycle mean (%)	60.2 ± 1.07	64.3 ± 1.28	0.021
Parameters	12 months-old		
Paw intensity measures	**WT**	***CMT2A Tg***	***P-value***
Right forepaw Max contact max intensity (a.u)	201.1 ± 1.9	191.9 ± 2.9	0.013
Right forepaw Max intensity mean (a.u)	205 ± 1.1	197.5 ± 2.2	0.005
Right forepaw Mean intensity (a.u)	93.7 ± 1.5	89.4 ± 1.1	0.025
Right forepaw Mean intensity of the 15 most intense pixels mean (a.u)	180.8 ± 3.2	169.7 ± 3.6	0.025
Right hindpaw Max intensity mean (a.u)	211.4 ± 1.2	203.5 ± 3.1	0.029
Left forepaw Max contact max intensity (a.u)	201.3 ± 1.7	193.5 ± 2.4	0.011
Left forepaw Max intensity mean (a.u)	205.2 ± 1	199.3 ± 1.9	0.013
Gait/Posture			
Left hindpaw Stand mean (sec)	0.21 ± 0.012	0.27 ± 0.02	0.047
Support three (%)	27.4 ± 2.8	36.5 ± 2.6	0.021
Coordination			
Phase dispersions Right forepaw> Right hindpaw mean (%)	51 ± 1.4	55.7 ± 1.5	0.027
Couplings Right forepaw> Right hindpaw mean (%)	50.9 ± 1.4	56.8 ± 1.7	0.012

Table S1. Catwalk locomotion parameters affected in *CMT2A Tg* mice
Summary of the parameters affected in 6 and 12 month-old *CMT2A Tg* mice (6 month-old: n=23; 12 month-old: n=17) compared to WT mice (6 month-old: n=18; 12 month-old: n=15). Parameters were classified according to paw intensity, paw size, gait/posture and coordination. Statistical analysis: two-tailed unpaired student's t-test.

References for SI reference citations

1. Cartoni R, *et al.* (2010) Expression of mitofusin 2(R94Q) in a transgenic mouse leads to Charcot-Marie-Tooth neuropathy type 2A. *Brain* 133(Pt 5):1460-1469.
2. Bernard-Marissal N, Medard JJ, Azzedine H, & Chrast R (2015) Dysfunction in endoplasmic reticulum-mitochondria crosstalk underlies SIGMAR1 loss of function mediated motor neuron degeneration. *Brain* 138(Pt 4):875-890.
3. Dirren E, *et al.* (2015) SOD1 silencing in motoneurons or glia rescues neuromuscular function in ALS mice. *Ann Clin Transl Neurol* 2(2):167-184.
4. Caballero-Garrido E, Pena-Philippides JC, Galochkina Z, Erhardt E, & Roitbak T (2017) Characterization of long-term gait deficits in mouse dMCAO, using the CatWalk system. *Behav Brain Res* 331:282-296.
5. Verhoeven K, *et al.* (2006) MFN2 mutation distribution and genotype/phenotype correlation in Charcot-Marie-Tooth type 2. *Brain* 129(Pt 8):2093-2102.
6. Schindelin J, *et al.* (2012) Fiji: an open-source platform for biological-image analysis. *Nat Methods* 9(7):676-682.
7. Gonzalez S, *et al.* (2015) In vivo time-lapse imaging of mitochondria in healthy and diseased peripheral myelin sheath. *Mitochondrion* 23:32-41.
8. Filezac de L'Etang A, *et al.* (2015) Marinesco-Sjogren syndrome protein SIL1 regulates motor neuron subtype-selective ER stress in ALS. *Nat Neurosci* 18(2):227-238.
9. Stoica R, *et al.* (2014) ER-mitochondria associations are regulated by the VAPB-PTPIP51 interaction and are disrupted by ALS/FTD-associated TDP-43. *Nat Commun* 5:3996.